Surface Reactions and Wetting Mechanisms of Titanium- and Aluminum-Containing Nickel-Base and Iron-Base Alloys During Brazing under Vacuum

Different thermal expansions at brazing temperature cause oxide, nitride and carbide surfaces on base metals to crack and allow filler metals to penetrate and wet the underlying base metals

BY E. LUGSCHEIDER, H. ZHUANG AND M. MAIER

Introduction

To obtain quality brazed joints, the perfect wetting of the parts being brazed is a necessity. Even relatively thin surface layers on base metals, particularly oxides, can cause insufficient wetting. A decisive factor in the separation of surface layers during brazing in vacuum is the stability of the surface structure; this is a function of the composition of the base metal.

On stainless steel, base metal surface wetting is attained by reducing the chromium oxide layer with carbon in the steel to produce carbon monoxide under vacuum of 10^{-4} to 10^{-5} mbar at temperatures above 900°C, *i.e.*, 1652°F (Ref. 1).

This paper discusses the temperature-dependent surface reactions of titanium- and aluminum-containing base metals under vacuum heat treatment. These elements develop extremely stable oxide, nitride, and carbide surface structures; the wetting behavior of high-temperature brazing filler metals on these materials during brazing under vacuum conditions is reported.

Based on a paper presented at the 13th International AWS-WRC Brazing and Soldering Conference held in Kansas City, Missouri, during April 27-29, 1982.

E. LUGSCHEIDER is Professor, Material Science Division, Technical University of Aachen; M. MAIER is with the Institute of Semiconductor Electronics, Technical University of Aachen, Federal Republic of Germany; and H. ZHUANG is Professor, Beijing Institute of Aeronautics and Astronautics, Beijing, China.

Test Procedure

The following base metals were investigated: a nickel-base alloy similar to Inconel 700 and a martensitic iron-base alloy. Both base metals were brazed with three high-temperature brazing filler metals – BNi-2, BNi-7, and BAu-4 (Table 1).

Temperature-dependent base metal surface reactions were tested during vacuum treatment. To accomplish this, samples polished and cleaned ultrasonically were annealed in a vacuum of 2×10^{-5} mbar (1.5×10^{-5} torr)* at temperatures up to 1150°C (2100°F). The wetting tests took place in a vacuum of 2×10^{-5} mbar at the recommended brazing temperatures.

The following methods of investigation were applied:

- Auger electron spectroscopy (AES) with sputter etching.
- Secondary ion mass spectrometry (SIMS).

**1 torr = 1.33 mbar*

Table 1—Composition of Base Metals and Brazing Filler Metals, Wt-%

	Base metals		Filler metals		
	Ni-alloy	Fe-alloy	BNi-2	BNi-7	BAu-4
C	<0.10	0.02	0.06	0.10	–
Cr	14.9	–	6.5	13.0	–
Al	1.8	–	–	–	–
Ti	1.8	1.6	–	–	–
Mo	2.9	4.0	–	–	–
Co	–	12.0	–	–	–
B	–	–	3.0	–	–
Si	–	–	4.5	0.1	–
P	–	–	–	10.0	–
Au	–	–	–	–	82.0
Fe	<0.5	Bal.	2.5	0.2	–
Ni	Bal.	18.0	Bal.	Bal.	18.0
BTR:[a]	–	–	1010-1175	925-1065	950-1005

(a) BTR = brazing temperature range in °C with °F equivalents as follows: 925°C = 1697°F; 950°C = 1742°F; 1005°C = 1841°F; 1010°C = 1850°F; 1065°C = 1949°F; 1175°C = 2147°F;

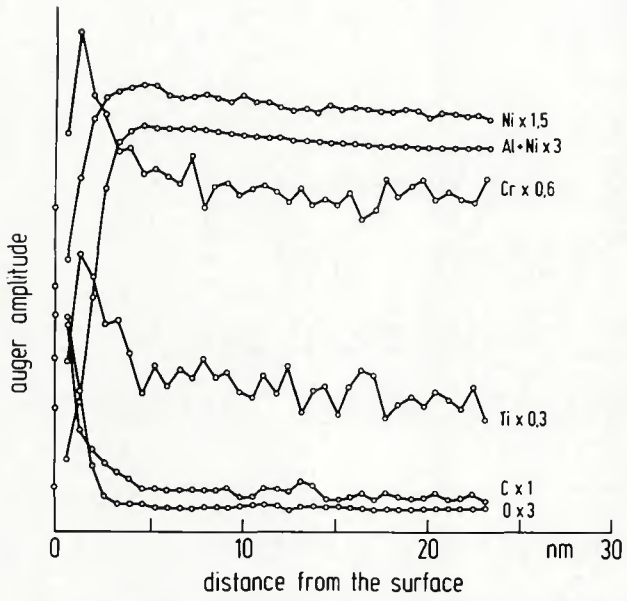

Fig. 1—AES depth profile of nickel-alloy base metal in purified as-supplied condition

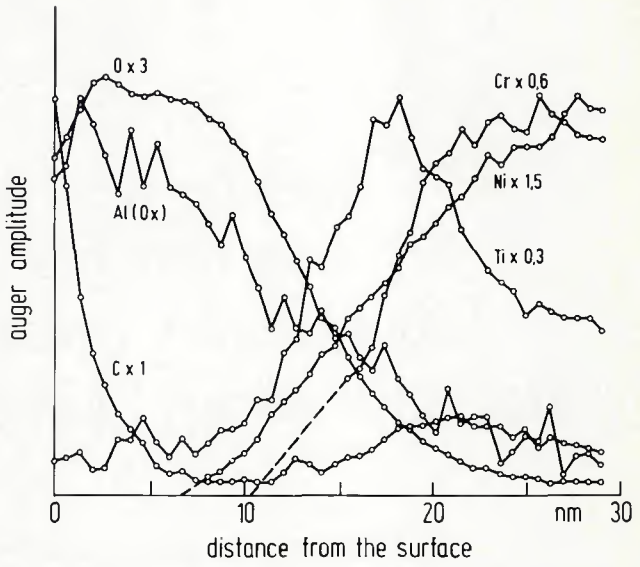

Fig. 2—AES depth profile of nickel-alloy base metal after vacuum annealing at 2 × 10^{-5} mbar and 1000°C (1832°F) for 10 min

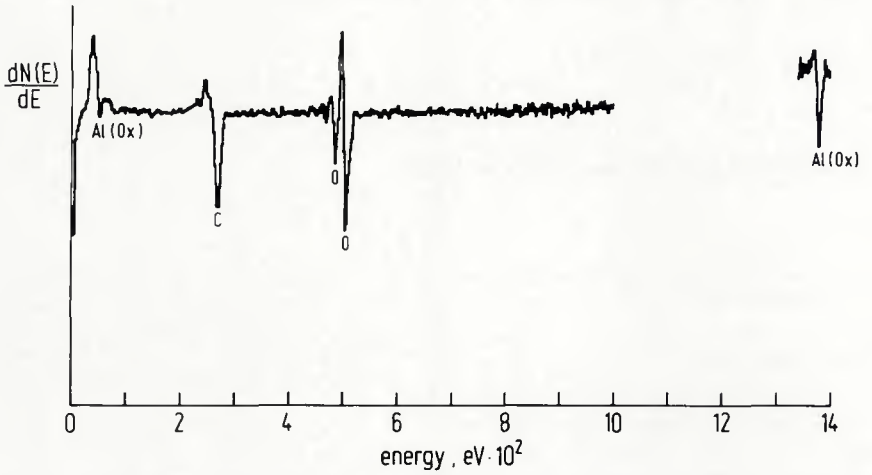

Fig. 3—Surface auger spectrum of nickel-alloy base metal after vacuum annealing at 2 × 10^{-5} mbar and 1000°C (1832°F) for 10 min

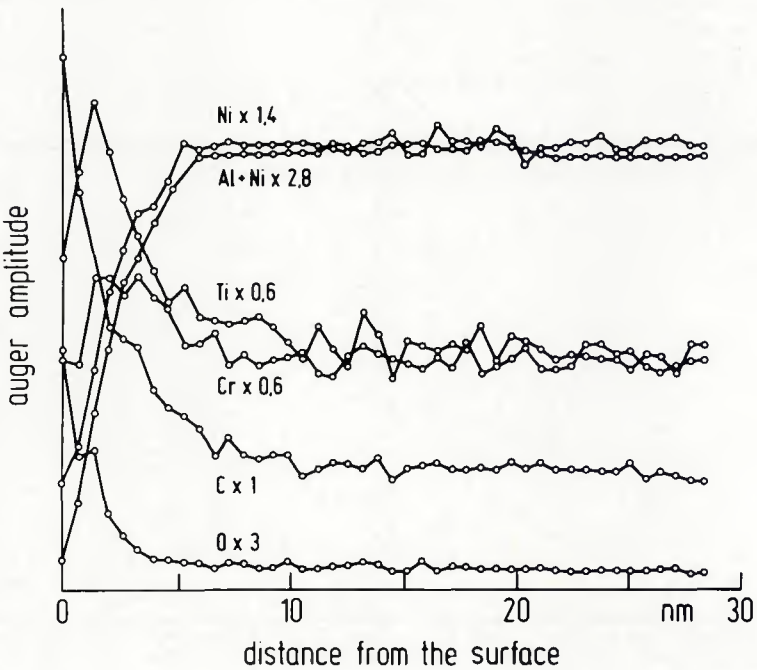

Fig. 4—AES depth profile of nickel-alloy base metal after vacuum annealing at 2 × 10^{-5} mbar and 1150°C (2100°F) for 10 min

- Scanning electron microscopy (SEM).
- Electron microprobe analysis (EMA).
- Thermogravimetry (TG).

Nickel-Alloy Base Metal

The AES surface analysis of the nickel-alloy base metal before heat treatment is shown in Fig. 1. To determine the depth profile of nickel, both high-energy (848 eV) and lower energy (61 eV) auger lines were applied. The latter coincides closely to that of aluminum. Molybdenum and iron were not determined. The "as-received" alloy was evidently carbon-contaminated. The surface layer had a thickness of approximately 2.5 nm (25 A°), and consisted not only of carbon, but also chromium, nickel, aluminum, titanium, and oxygen.

After vacuum annealing for 10 minutes (min) at 1000°C (1832°F) the nickel-alloy base metal had an almost metallic shine. The AES (depth profile of the sample) showed an increase to approximately 20 nm (200 A°) in the thickness of the base metal's surface layer—Fig. 2. The exterior layer area was free of nickel and chromium; however, carbon contamination as well as high aluminum and oxygen contents were recorded. An increase in titanium and carbon concentration was observed in a lower zone.

The auger-spectrum of the surface also shows a layer of aluminum oxide at 1378 eV—Fig. 3.

After vacuum annealing for 10 min at 1150°C (2100°F), the nickel-alloy base metal sample had a clear metallic shine; and the AES depth profile (Fig. 4) showed

a reduction of the base metal surface layer thickness to about 5 nm. The layer now containing nickel and chromium showed an increased titanium and carbon content. Conspicuous is the distinct reduction of the oxygen and aluminum concentration, evidenced by the lack of surface Al_2O_3 after annealing at 1000°C (1832°F). Thermogravimetrical measurement (Fig. 5) of the nickel-alloy base metal showed that a distinct reduction in weight is the consequence of annealing in a vacuum of 2×10^{-5} mbar at 1130°C (2066°F).

The evaporation of Al_2O_3 at these temperatures and pressures is not possible. Therefore, the question that must be considered is this: Can the aluminum-oxide in the surface be reduced by the carbon of the base material, as is the case in Cr_2O_3 coatings on stainless steel?

Theoretically, the reduction of Al_2O_3 by carbon corresponding to the reaction $3\ C + Al_2O_3 = 2\ Al + 3\ CO$ is possible. The free enthalpy $\Delta\ G_T$ of the chemical reaction is −12758 calories (cal.) for a temperature of 1150°C (2100°F) and a pressure of 10^{-7} atm. A reduction to volatile aluminum suboxide by the reaction, $2\ C + Al_2O_3 = Al_2O + 2\ CO$ is more likely due to the low carbon content. The $\Delta\ G_T$ value for this reaction at a temperature of 1150°F (2100°F) and a pressure of 10^{-7} atm. is −21465 cal. Even with a carbon activity of 0.001, the $\Delta\ G_T$ is still −8300 cal.

To experimentally test this hypothesis, a mixture of aluminum oxide (Al_2O_3) and carbon powder was heated at 1150°C (2100°F) under a vacuum of 2×10^{-5} mbar for 1 hour (h) in a steel sheet covered melting pot. The steel lid vaporized. The vaporization product could be clearly identified as an aluminum-oxygen product with the aid of AES analysis.

The absence of an Al_2O_3 surface layer on the nickel-alloy base metal annealed in a vacuum at 1150°C, *i.e.*, 2100°F (Fig. 4) can, therefore, be attributed to aluminum-suboxide volatilization due to carbon reduction.

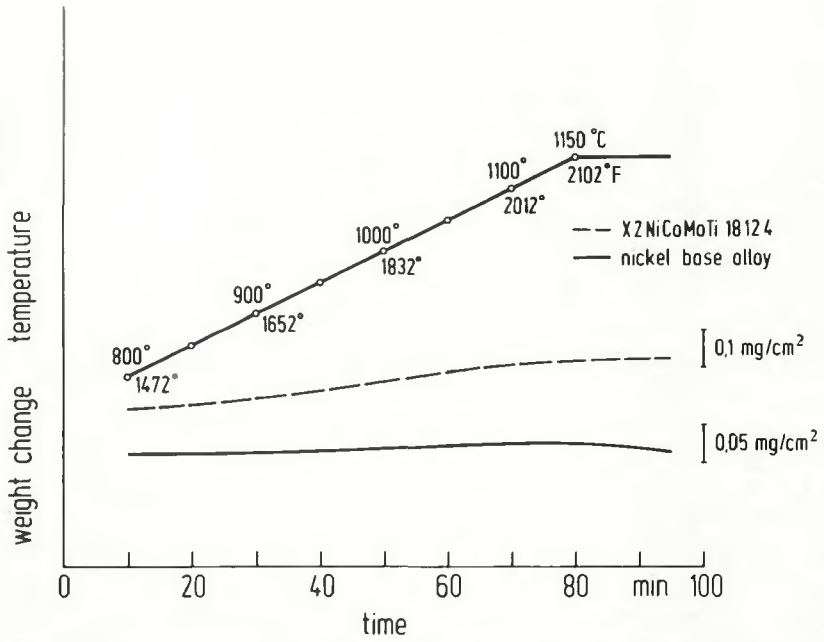

Fig. 5 — Temperature-dependent weight alteration of the surfaces of nickel- and iron-alloy base metals under annealing treatments in a 2×10^{-5} mbar vacuum

Iron-Alloy Base Metal

The surface layer thickness of the iron-alloy base metal was approximately 2.5 nm when supplied in a purified condition. The AES depth profile in Fig. 6 shows heavy carbon contamination as well as nickel, iron, titanium, and oxygen. The surface layer increased by about 90 nm after heat treatment under vacuum at 1000°C (1832°F) for 10 min. The AES depth profile showed a distinct increase in oxygen, carbon, and titanium concentration in the exterior layers — Fig. 7.

The absence of iron and nickel in the base metal surface layer was also demonstrated clearly in the auger-spectrum — Fig. 8. A SIMS analysis showed that, after 10 min vacuum annealing at 1000°C (1832°F), the surface layer of the iron-alloy base metal was composed of titanium carbide, nitride, and oxide — Fig. 9. These were also noted by the light yellow coloring of the sample.

The high aluminum peak shown in Fig. 9 was attributed to residual Al_2O_3 polishing compound on the surface as well as the sensitivity of the SIMS analysis to this element. Vacuum annealing at 1150°C (2100°F) caused obvious growth

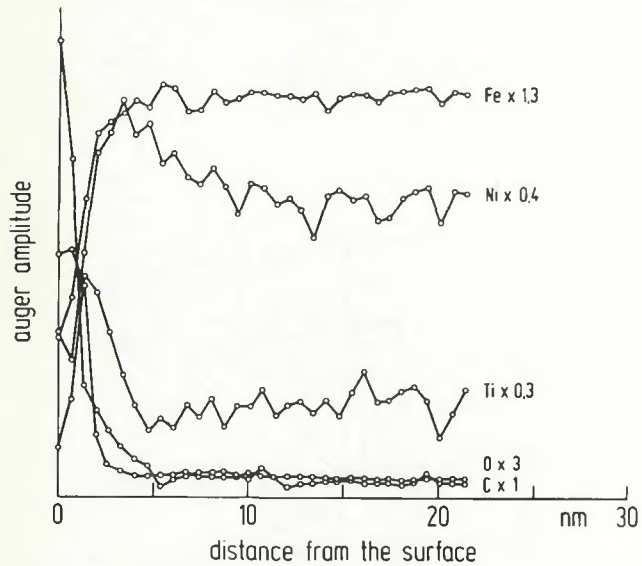

Fig. 6 — AES depth profile of iron-alloy base metal in purified as-supplied condition

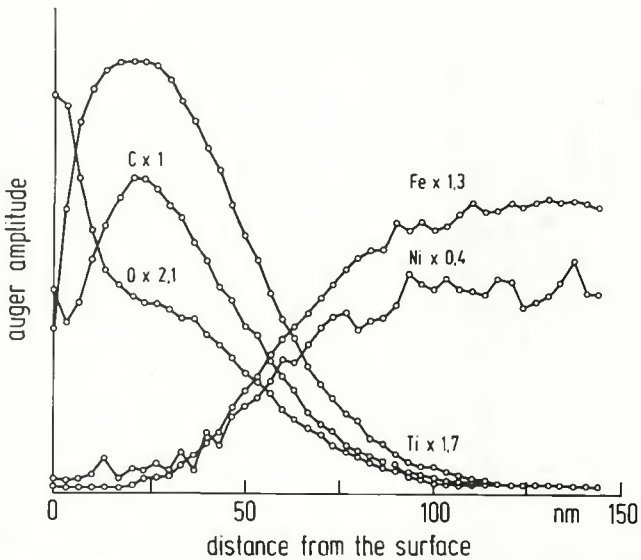

Fig. 7 — AES depth profile of iron-alloy base metal after vacuum annealing at 2×10^{-5} mbar and 1000°C (1832°F) for 10 min

in the titanium compound surface layer of the iron-base alloy—Figure 10. This did not occur on the nickel-alloy base metal. In addition, heat treatment at 1150°C (2100°F) led to distinct diffusion of iron and nickel in the iron-alloy base metal surface layer.

The constant increase in weight of the iron-alloy base metal with increased temperature, mainly due to the titanium reaction with residual gas of the vacuum, is demonstrated by the vacuum thermogravimetry results—Fig. 5. The surface of the sample shows a dark yellow coloring at 1150°C (2100°F).

Wetting Tests

Tests were conducted to determine the wetting behavior of the nickel- and iron-alloy base metals for high temperature brazing filler metals. To this end, filler metal coatings were brazed on base materials with filler metals BAu-4 and BNi-7 at 1000°C (1832°F) and with BNi-2 at 1040°C (1904°F). The brazing time was 15 min, and the pressure was below 2×10^{-5} mbar. Satisfactory wetting of the materials with small wetting angles was observed—Fig. 11. However, under these brazing conditions, the nickel-alloy base metal was coated with an aluminum oxide layer, and the iron-alloy base metal with a titanium nitride, titanium oxide, titanium carbide layer.

The base metal surface layers cracked at high temperatures, apparently because of the substantial difference in thermal expansion of the surface layer and the base metal. The filler metals could thus penetrate into the cracks and wet the underlying base metals. The AES analysis showed that the oxide, nitride, and carbide layers then floated up through the liquid filler metals.

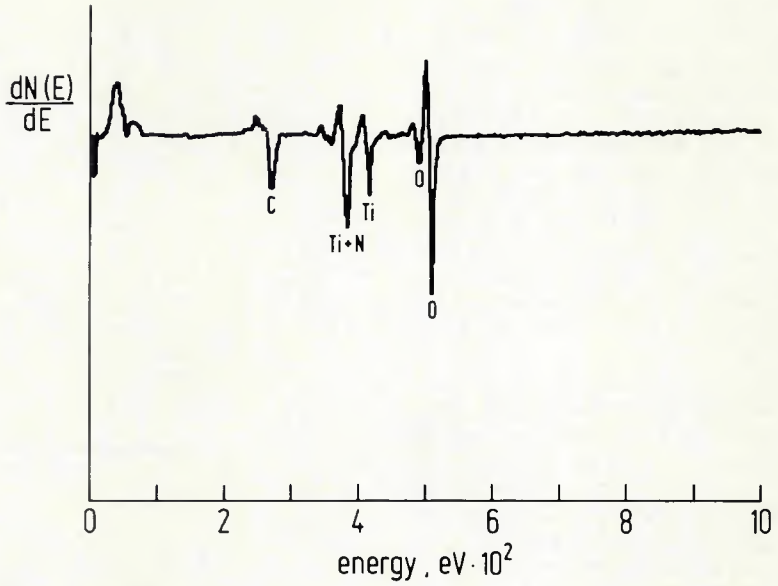

Fig. 8—Auger spectrum of the iron-alloy base metal surface after vacuum annealing at 2×10^{-5} mbar and 1000°C (1832°F) for 10 min

Almost the same auger spectrum was registered on the surface of the BAu-4 filler metal after application to the nickel-alloy base metal (Fig. 11B) as was found on the base metal after vacuum anneal for 10 min at 1000°C, *i.e.*, 1832°F (Fig. 3). It was mainly aluminum oxide. After the wetting of the iron-alloy base metal, the auger spectrum of the surface of the BAu-4 filler metal (Fig. 11E) showed the line pattern typical of appropriately heat-treated base materials—Figs. 8 and 12. Titanium compounds prevailed, and gold from the filler metal was absent.

Metallographic investigation of base metal surface layers that floated upward in liquid filler metal and their presence on the filler metal surface was carried out by brazing both the nickel- and iron-alloy base metals with a coating of BNi-7 filler metal. To gain thicker surface layers, the base metals were systematically preoxidized before brazing under vacuum at 2×10 mbar and 1000°C (1832°F). This was done by annealing the nickel-alloy base metal for 1 h at 1000°C (1832°F) in a vacuum of 10^{-2} mbar and the iron-alloy base metal for 10 min at 1150°C (2100°F) in a vacuum of 10^{-4} mbar.

Micrographs, in Fig. 13, of the BNi-7 filler metal brazed on both base metals showed distinct upward floating of base metal surface layers and reduced wetting of the filler metal. The microprobe analysis of the elements at the BNi-7/nickel-alloy base metal and BNi-7/iron-alloy base metal interfaces (Fig. 14) showed distinct increases in the aluminum and oxygen concentration (Fig. 14A) and in

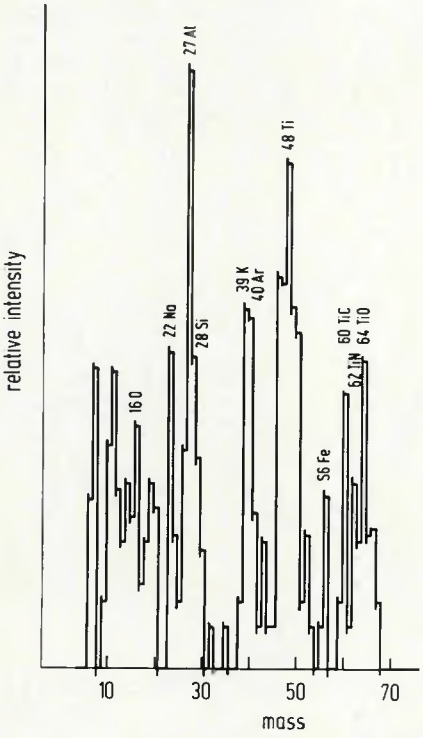

Fig. 9—SIMS analysis of the iron-alloy base metal surface after vacuum annealing at 2×10^{-5} and 1000°C (1832°F) for 10 min

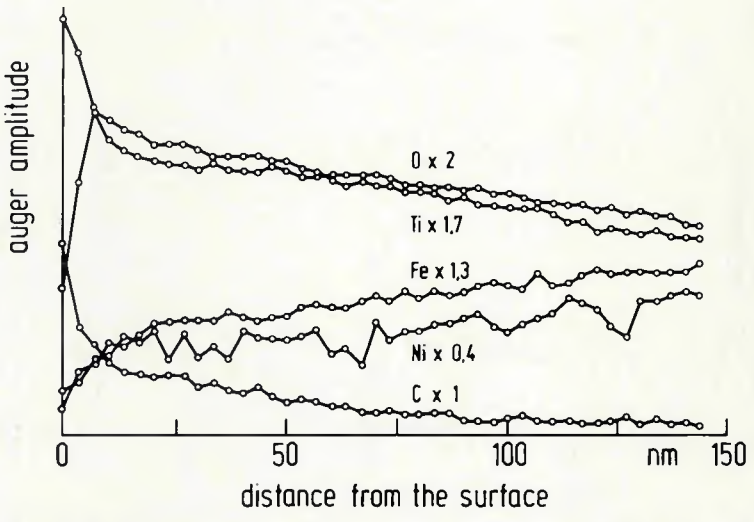

Fig. 10—AES depth profile of the iron-alloy base metal after vacuum annealing at 2×10^{-5} mbar and 1150°C (2100°F) for 10 min

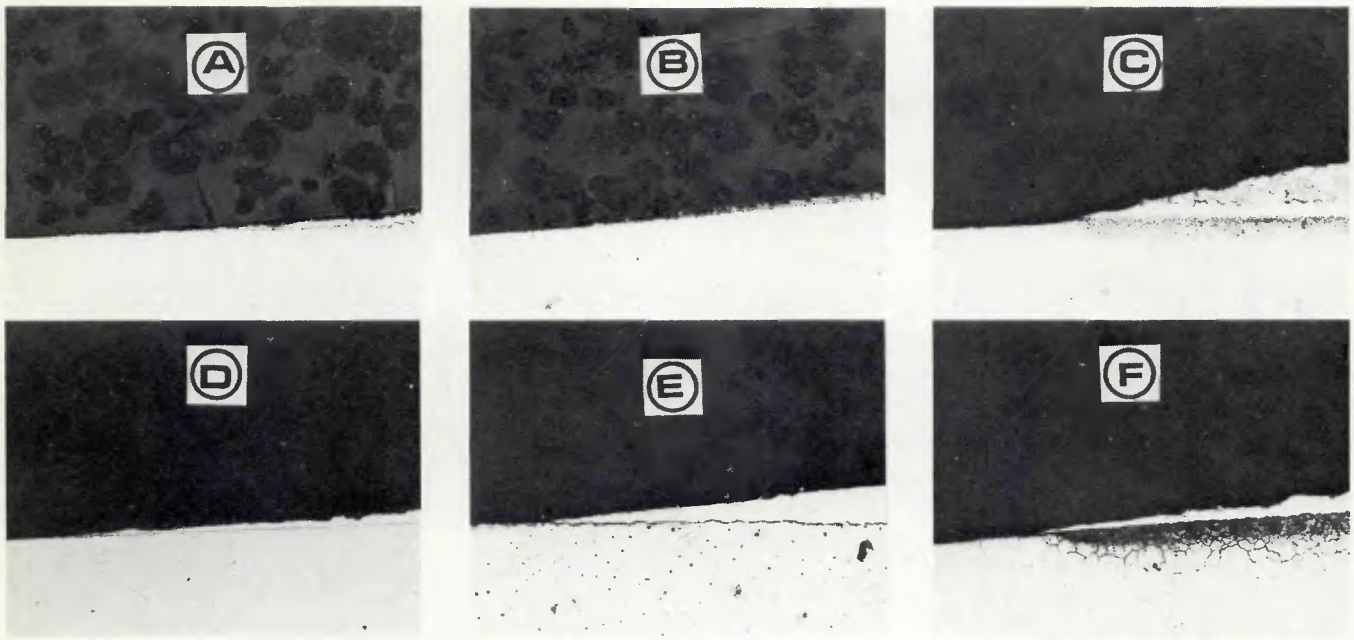

Fig. 11 — Micrographs of various filler metals after being brazed under vacuum for 10 min at 2 X 10^{-5} mbar onto the surfaces of nickel- and iron-alloy base metals: A — BNi-7 on Ni-alloy base metal, 1000°C; B — BAu-4 on Ni-alloy base metal, 1000°C; C — BNi-2 on Ni-alloy base metal, 1040°C; D — BNi-7 on Fe-alloy base metal, 1000°C; E — BAu-4 on Fe-alloy base metal, 1000°C; F — BNi-2 on Fe-alloy base metal, 1040°C (note: 1000 and 1040°C equivalent to 1832 and 1904°F, respectively). X50

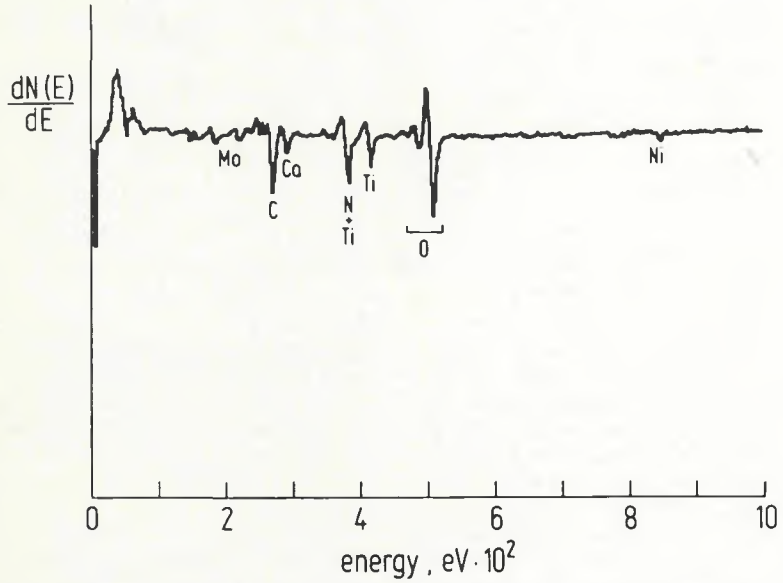

Fig. 12 — Auger spectrum of BAu-4 filler metal surface after being brazed under vacuum on iron-alloy base metal at 2 X 10^{-5} mbar and 1000°C (1832°F) for 10 min

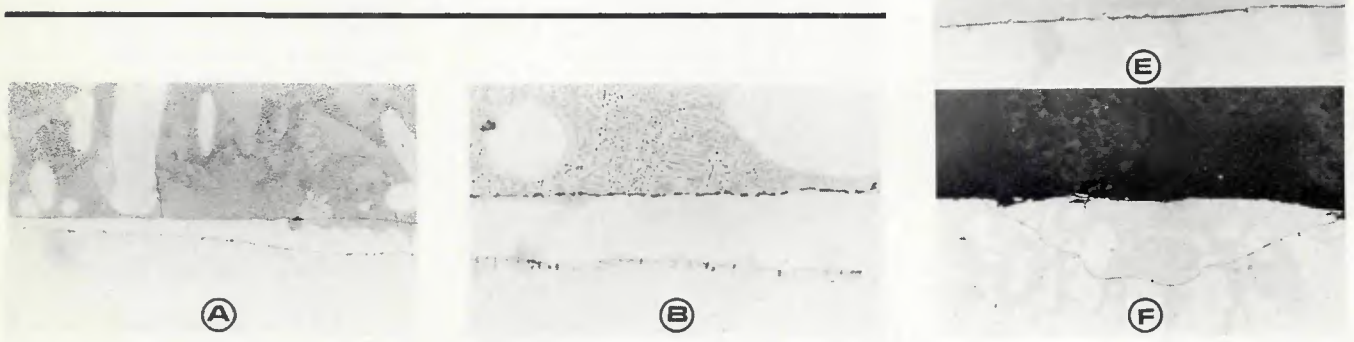

Fig. 13 — BNi-7 filler metal after being brazed under vacuum onto the surfaces of nickel- and iron-alloy base metals at 2 X 10^{-5} mbar and 1000°C (1832°F): A — Fe-alloy base metal, 10 min, X200; B — Fe-alloy base metal, 10 min, X500; C — Fe-alloy base metal, 15 min, X200; D — Ni-alloy base metal, 10 min, X200; E — Ni-alloy base metal, 10 min, X500; F — Ni-alloy base metal, 15 min, X200 (reduced 68% on reproduction)

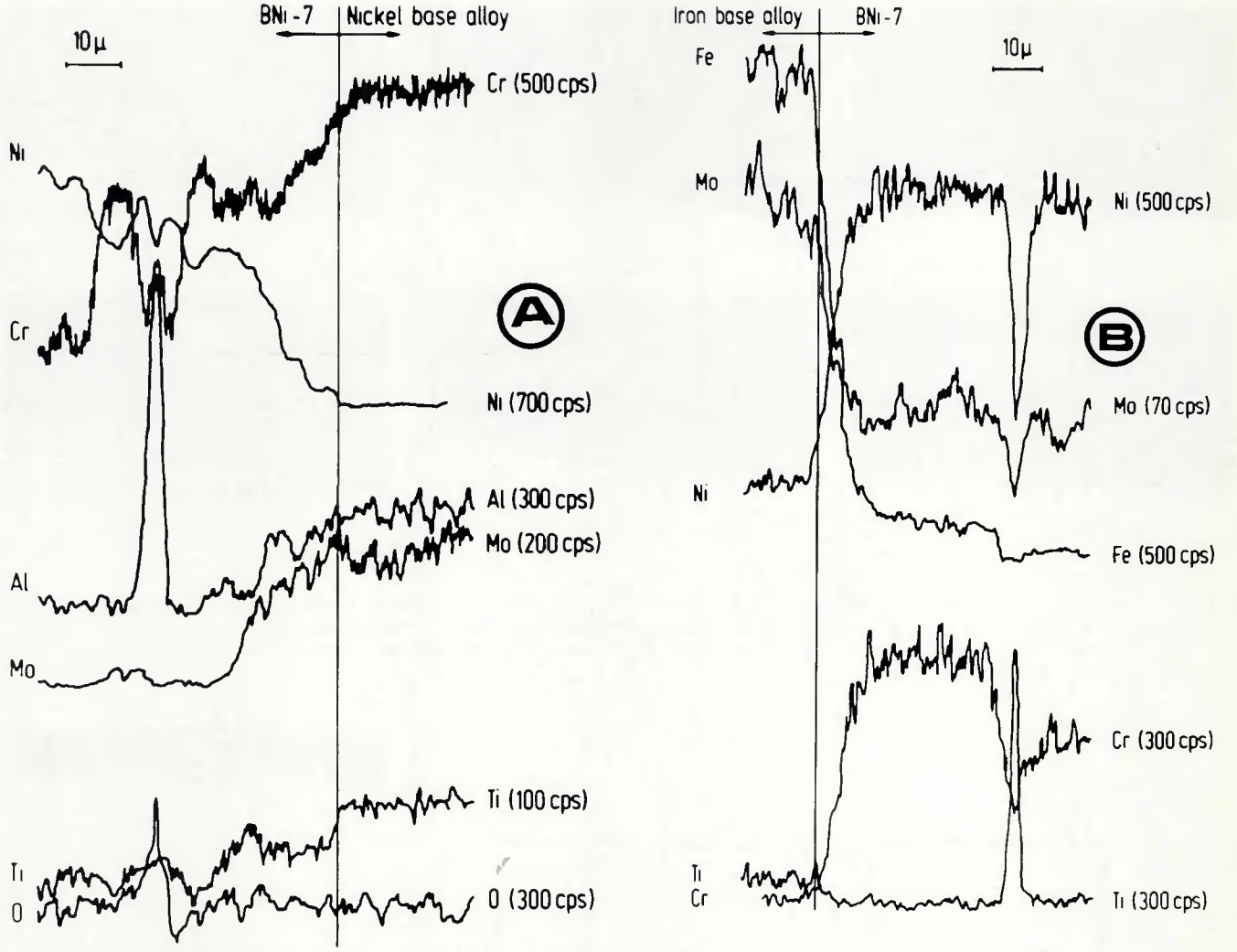

Fig. 14—Microprobe analysis on the alloy element distribution following the brazing under vacuum of BNi-7 filler metal on two base metals at 2 × 10^{-5} mbar and 1000°C (1832°F) for 10 min: A—Ni-alloy base metal; B—Fe-alloy base metal

the titanium concentration (Fig. 14B).

The penetration of BAu-4 high temperature filler metals into the cracks of the surface layers of the nickel- and iron-alloy base metals during brazing, with subsequent wetting of the base metal, can also be observed in the scanning electron microscope graphs. Figure 15 shows a fissured surface structure, almost the same in both filler metal and base metal, at the transition zone between the braze coating and base metal.

Summary

During brazing in vacuum (2 × 10^{-5} mbar) of nickel alloys containing titanium and aluminum, the formation of base metal surface layers is extremely temperature-dependent. A constant growth in the thickness of the predominantly aluminum oxide surface layer was observed at temperatures up to approximately 1130°C (2066°F). Above approximately 1150°C (2100°F), the aluminum oxide was reduced to aluminum suboxide by the base metal carbon; the remaining layer consisted mainly of titanium compounds and was about as thick as was the original layer before heat treatment.

A titanium-containing iron-alloy base metal heat-treated under the same vacuum conditions showed a constant increase in the thickness of its surface layer with increasing temperatures. The surface layer was predominantly composed of titanium oxide, nitrides, and carbides.

Brazing tests in a 2 × 10^{-5} mbar vacuum were conducted with BNi-2, BNi-7 and BAu-4 filler metals at temperatures of 1000 and 1040°C (1832 and 1904°F). Results showed that wetting of the base metal takes place despite surface layer formation. Due to the differing thermal expansions at brazing temperature, the oxide, nitride and carbide surface layers on the base metal crack and allow the filler metal to penetrate and wet the base metal. The surface layers then start to float up through and on the liquid filler metals. Nevertheless, difficulties in filling small brazing clearances and nonmetallic inclusions in the brazed joint do reduce joint strength and should be taken into consideration.

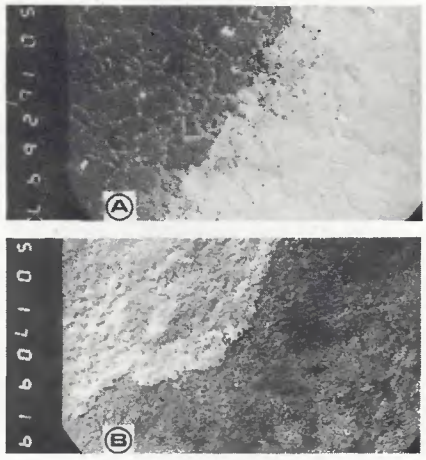

Fig. 15 (right)—SEM micrograph of the transition zone of BAu-4 filler metal/base metal following brazing under vacuum at 2 × 10^{-5} mbar and 1000°C (1832°F) for 10 min: A—Ni-alloy base metal, X500; B—Fe-alloy base metal, X430 (A and B reduced 53% on reproduction)

Reference

1. Lugscheider, E., and Zhuang, H. 1982. *Schweissen und Schneiden* 34:490.